# Palaeoglacial and palaeoclimatic conditions in the NW Pacific, as revealed by a morphometric analysis of cirques upon the Kamchatka Peninsula

**Iestyn D. Barr**[a] **& Matteo Spagnolo**[b]

[a]School of Geography, Archaeology and Palaeoecology, Queen's University Belfast, BT7 1NN, Belfast, UK
Email: i.barr@qub.ac.uk

[b]School of Geosciences, University of Aberdeen, Elphinstone Road, AB243UF, Aberdeen, UK

---

This is an author produced version of a paper published in **Geomorphology**

---

## Published paper

Barr, ID., Spagnolo, M. (2013). Palaeoglacial and palaeoclimatic conditions in the NW Pacific, as revealed by a morphometric analysis of cirques upon the Kamchatka Peninsula. *Geomorphology,* 192. 15-29. doi:10.1016/j.geomorph.2013.03.011

http://www.sciencedirect.com/science/article/pii/S0169555X13001529

**Palaeoglacial and palaeoclimatic conditions in the NW Pacific, as revealed by a morphometric analysis of cirques upon the Kamchatka Peninsula**

**Iestyn D. Barr (Corresponding author)**
School of Geography, Archaeology and Palaeoecology, Queen's University Belfast, BT7 1NN, Belfast, UK
Email: i.barr@qub.ac.uk
Tel: +44 (0)28 9097 5146

**Matteo Spagnolo**
School of Geosciences, University of Aberdeen, Elphinstone Road, AB243UF, Aberdeen, UK

**Keywords**
Kamchatka
Cirques
Morphometry
Climate
Glaciation

**Abstract**
The distribution of glacial cirques upon the Kamchatka peninsula, Far Eastern Russia, is systematically mapped from satellite images and digital elevation model data. A total of 3,758 cirques are identified, 238 of which are occupied by active glaciers. The morphometry of the remaining 3,520 cirques is analysed. These cirques are found to show a very strong N bias in their azimuth (orientation), likely resulting from aspect-related variations in insolation. The strength of this N bias is considered to indicate that former glaciation upon the peninsula was often 'marginal', and mainly of cirque-type, with peaks extending little above regional equilibrium-line altitudes. This is supported by the fact that S and SE-facing cirques are the highest in the dataset, suggesting that glacier-cover was rarely sufficient to allow S and SE-facing glaciers to develop at low altitudes. The strength of these azimuth-related variations in cirque altitude is thought to reflect comparatively cloud-free conditions during former periods of glaciation. It is suggested that these characteristics, of marginal glaciation and comparatively cloud-free conditions, reflect the region's former aridity, which was likely intensified at the global Last Glacial Maximum, and during earlier periods of ice advance, as a result of the development of negative pressure anomalies over the North Pacific (driven by the growth of the Laurentide Ice Sheet), combined with other factors, including an increase in the extent and duration of sea ice, a reduction in global sea levels, cooler sea surface temperatures, and the localised growth of mountain glaciers. There is published evidence to suggest extensive glaciation of the Kamchatka Peninsula at times during the Late Quaternary, yet the data presented here appears to suggest that such phases were comparatively short-lived, and that smaller cirque-type glaciers were generally more characteristic of the period.

## 1. Introduction

Glacial cirques are semi-circular hollows, open in downslope directions, and bounded upslope by steep headwalls. They are ubiquitous in many of the world's mountain ranges, and reflect the action of glaciers in eroding landscapes over tens to hundreds of thousands of years (Evans, 2006a). Cirques have long been used as direct indicators of the extent and nature of former glaciation, and therefore as indicators of palaeoclimate (e.g. Evans, 1977; Aniya and Welch, 1981; Evans and Cox, 1995; García-Ruiz et al., 2000; Federici and Spagnolo, 2004; Evans, 2006a; Hughes et al., 2007; Ruiz-Fernandez et al., 2009). They are useful for this purpose because their distribution, morphometry and orientation (azimuth) are influenced by the intensity, duration and extent of glaciation, which are, in turn, driven by climate and topography (amongst other factors). This link to palaeoclimate is particularly relevant because cirques often occupy remote and inaccessible regions (i.e. mountainous environments), where other palaeoenvironmental proxies may be limited or lacking. The focus of this investigation is to utilise cirques, in the way noted above, to investigate palaeoglacial and palaeoclimatic conditions upon the Kamchatka Peninsula, Far Eastern Russia. This is a region which plays and (likely) played a key role in regulating climatic conditions across the North Pacific (see Yanase and Abe-Ouchi, 2007, 2010; Otieno et al., 2012), yet where very little is known about former climate, especially during the last main glaciation (see Barr and Clark, 2011, 2012b). Part of the uncertainty regarding former conditions upon the Kamchatka Peninsula, relates to a general lack of

investigation, at least partly because of the region's inaccessibility. Fortunately, the recent availability of remote sensing data, particularly digital elevation models (DEMs) and satellite images, has opened up the region to investigation. In the present study, we make use of these remotely-sensed sources to systematically map glacial cirques across the Kamchatka Peninsula for the first time. The area under investigation is roughly 270,000 km$^2$, and a total of 3,758 cirques are mapped—constituting one of the largest populations ever investigated. GIS-techniques are employed to analyse variations in cirque morphometry (size, shape and altitude), azimuth, and insolation (annual, summer and winter). In so doing, the intention is to gain an improved understanding of palaeoglacial and palaeoclimatic conditions in this remote and little-investigated region, where the nature of former glaciation is poorly-understood, and where palaeoclimatic data are scarce.

## 2. Previous cirque investigations

The investigation of cirque formation, distribution and/or morphometry has a strong heritage, extending back to the late 19$^{th}$ Century (e.g. Helland, 1877; Harker 1901). Many of these earlier studies are summarised by Evans (1977), who provides details of 58 globally-distributed investigations, comprising a total population of ~9,600 cirques. Details of some more recent investigations are provided in table 1. Neither this dataset, nor the one presented by Evans (1977) are exhaustive, but detail some of the largest and most significant investigations (i.e. those where cirques, specifically, are the focus), many of which are built upon a number of smaller studies. It is apparent, from the summary provided by Evans (1977) and from the data presented here (see table 1), that investigations have largely focused upon Europe and North America, though isolated studies have been conducted elsewhere (e.g. New Zealand, Antarctica, Australia, Japan) (see figure 1). Some areas, particularly Britain, and North America, have been investigated on a number of occasions. However, there are many other areas globally which remain comparatively unexplored, including much of South America, Central Asia, and Eastern Russia (see figure 1). These are vast regions that have the potential of including large numbers of cirques whose study might substantially contribute to our understanding of the processes behind cirque formation, as well as enhancing our knowledge of palaeoclimatic conditions across the Earth.

*Table 1. Details of some recent investigations of cirque distribution and/or morphometry.*

| Citation | Region | Number cirques | L (range) | L (mean) | W (range) | W (mean) | H (range) | H (mean) |
|---|---|---|---|---|---|---|---|---|
| Křížek et al (2012) | Czech Republic, Germany, Poland | 27 | 278-1798 | 788 | 360-1467 | 700 | 116-453 | 272 |
| Anders et al (2010) | Switzerland | 500 | | | | | | |
| Mîndrescu et al (2010) | Romania | 631 | | 654 | | 718 | | 209 |
| Stauch and Lehmkuhl (2010) | NE Russia | 498 | | | | | | |
| Ruiz-Fernández et al (2009) | Spain (WMPE) | 59 | 125-475 | 295 | 125-1375 | 467 | 119-530 | 294 |
| | Spain (SSWA) | 70 | 125-950 | 487 | 250-2000 | 594 | 57-423 | 255 |
| Hughes et al (2007) | Greece | 35 | 200-2675 | 787 | 250-1550 | 662 | 100-600 | 331 |
| Steffanová and Mentlík (2007) | Czech Republic, Germany | 7 | 677-1237 | 1040 | 608-1352 | 949 | 187-385 | 287 |
| Marinescu (2007) | Romania | 10 | 839-1727 | 1172 | 589-2549 | 1124 | 230-490 | 358 |
| Brook et al (2006) | New Zealand | 92 | | | | | | |
| Evans (2006a) | Wales | 260 | 215-2750 | 667 | 235-2397 | 772 | 43-686 | 236 |
| Chueca and Julian (2004) | Spain | 3 | | | | | | |
| Federici and Spagnolo (2004) | France, Italy | 432 | 233-2410 | 672 | 211-2906 | 663 | 87-1328 | 355 |
| Ureda (2001) | Romania | 31 | 400-1975 | 879 | 275-1600 | 727 | 130-530 | 294 |
| García-Ruiz et al. (2000) | Spain | 206 | 100-1600 | 519 | 200-2700 | 691 | 100-943 | 364 |
| Evans (1999) | Wales | 228 | | | | | | |
| Davis (1999) | USA | 49 | 610-3505 | 1687 | 455-1900 | 954 | 190-760 | 442 |
| Hassinen (1998) | Norway, Sweden, Finland | 539 | 150-4000 | 845 | 250-3100 | 888 | 90-1180 | 400 |
| Evans and Cox (1995) | England | 158 | 220-1830 | 620 | 215-1700 | 680 | 75-580 | 241 |
| Evans (1994) | Canada | 198 | | 798 | | 749 | | 288 |
| Rudberg (1994) | Norway, Sweden | 4000+ | | | | | | |
| Embleton and Hamann (1988) | Austria and UK | 302 | | | | | | |
| Vilborg (1984) | Sweden | >200 | | | | | | |
| Aniya and Welch (1981) | Antarctica | 56 | 660-4584 | 2116 | 840-3240 | 1679 | 314-515 | 849 |
| Olyphant (1981) | USA | 23 | | | | | | |

Investigations conducted, thus far, vary considerably in terms of the number of cirques analysed. Some are based upon fewer than ten cirques (e.g. Sharp et al., 1959; Steffanová and Mentlík; 2007), though most populations comprise between ten and 250. To our knowledge, only two investigations have considered populations of more than 1,000 cirques: Péwé et al. (1967), who present a population of 1,474 cirques in Alaska; and Rudberg (1994), who considers more than 4,000 Scandinavian cirques.

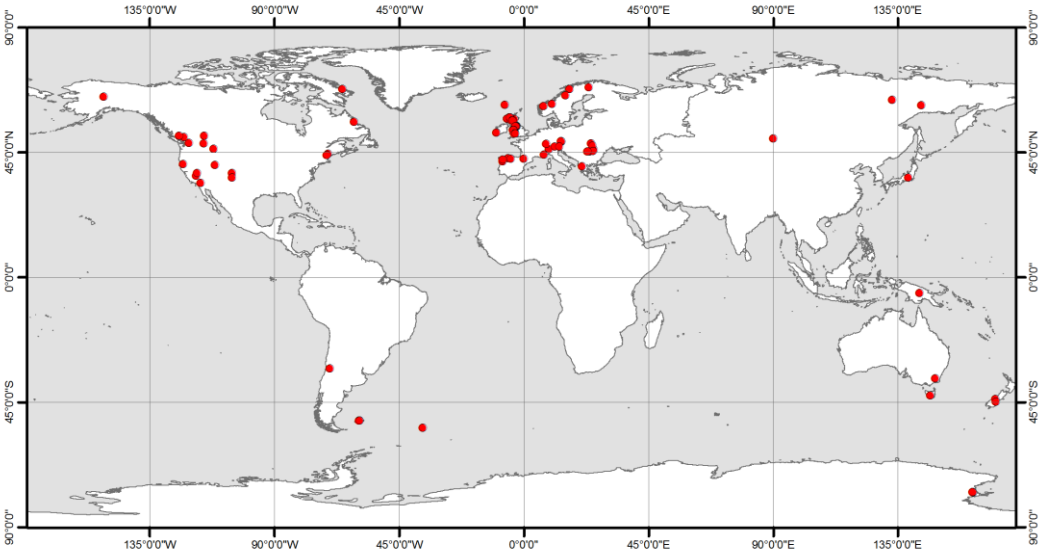


*Figure 1. Location of previous cirque investigations outlined in Evans (1977) and in table 1. In total, the locations of 84 investigations are presented. This map does not represent all previous investigations, but focuses upon some of the largest and most significant databases. [This figure is to be reproduced in colour on the Web (free of charge) and in black-and-white in print]*

## 3. Study area

### 3.1. Topography and tectonics

The Kamchatka Peninsula extends from NE to SW, for approximately 1,250 km and separates the Sea of Okhotsk to the W from the North Pacific to the S and E (figure 2). The peninsula's topography is dominated by three key mountain groups: the Sredinny Mountains; the Vostočny Mountains; and the Eastern Volcanic plateau (see figure 2). . The peninsula is one of the most volcanically-active arc segments on Earth (Bindeman et al., 2010), and is currently occupied by 29 active, and ~300 extinct volcanoes (Solomina et al., 2007), the highest of which reaches 4,750 m above sea level (a.s.l.). This volcanic activity is driven by proximity to the Kurile-Kamchatka trench, where the Pacific Plate subducts beneath the Eurasian Plate, at an average rate of 79 mm $yr^{-1}$ (DeMets et al., 1990). During the Late Eocene, this subduction zone, and volcanic front was located in the Sredinny Mountains (Bindeman et al., 2010), and has since migrated east (Bindeman et al., 2010), to its present location, ~150 km off the eastern shore of the peninsula (see figure 2). This migration resulted in the formation of the Sredinny Mountains, the volcanoes of the Central Kamchatka Depression, and finally the Vostočny Mountains and Eastern Volcanic Plateau (Bindeman et al., 2010). Thus, these mountain complexes become successively younger from west to east, with volcanoes of the Sredinny Mountains largely active during the Late Quaternary and Holocene, and active volcanoes now mostly found in the Vostočny Mountains and upon the Eastern Volcanic plateau (Ivanov, 2002). Given this volcanic activity, much of the Peninsula has undergone uplift and deformation during the past 70 Ma or more (Fedotov et al., 1988), yet direct estimates of this uplift are few. Upon the Kamchatskiy Peninsula (see boxed area 'A' in figure 2), published estimates suggest Miocene-Quaternary uplift rates of 0.14 to 1.38 mm $yr^{-1}$ (Freitag et al., 2001), with Late Quaternary rates ranging from 0.1 to 1.0 mm $yr^{-1}$ (Pedoja et al., 2004). Estimates from the Ozernoi Peninsula (see boxed area 'B' in figure 2), suggest Quaternary uplift rates of 0.1–0.3 mm $yr^{-1}$ (Pedoja et al., 2006), whilst estimates from the SE flanks of the Sredinny Mountains (see boxed area 'C' in figure 2) suggest uplift rates of 0.18 to 0.67 mm $yr^{-1}$ from the Late Oligocene to the present (Hourigan et al., 2004). Given these estimates, it is recognised that uplift might have created an artificial offset in the altitude of cirques analysed in the present study. For example, with the maximum suggested rate of 1.38 mm $yr^{-1}$, 100 ka –old cirques initially formed at 1,000 m (a.s.l.) would now be found at an elevation of 1,138 m (a.s.l). However, if the minimum suggested rate is applied, then these same cirques would only be a few meters higher than their origin. Though we acknowledge that in a 'maximum-suggested-rate' scenario the offset in cirque altitudes would have some (but limited) impact upon our interpretations, uplift

rates are likely to have varied both spatially and temporally during the past 100 ka, and lack of knowledge about these details prevents us from making any correction for uplift within the present study.

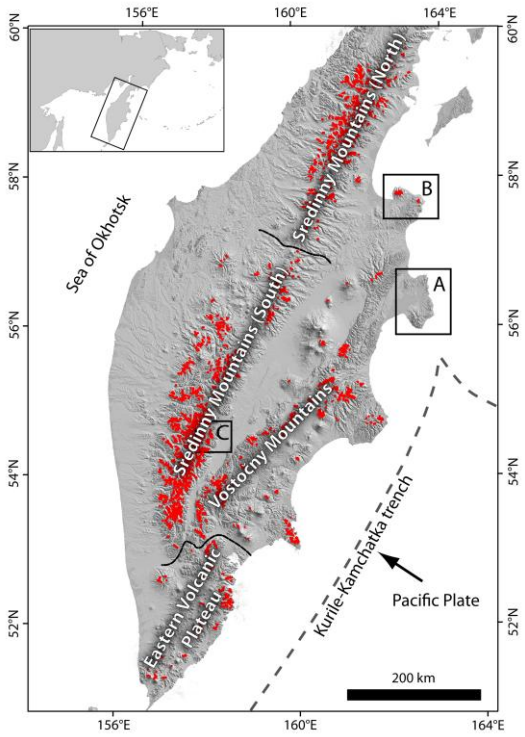


*Figure 2. Map of the Kamchatka Peninsula, showing the principal topographic regions referred to in the text. Points (red dots) correspond to 3,758 mapped cirques. The current location of the Kurile-Kamchatka trench, where the Pacific Plate subducts beneath the Eurasian Plate, is also shown. Boxed areas A-C are referred to in the text. [This figure is to be reproduced in colour on the Web (free of charge) and in black-and-white in print]*

### 3.2. Climate

At present, there are 15 permanent active weather stations upon the Kamchatka Peninsula, but only six provide consistent temperature and precipitation data over recent decades (none of which provide data representative of the region's mountain climates). A small number of temporary weather stations have been installed in mountainous regions, but these have only been used to monitor conditions during specific periods, typically covering fewer than two years (e.g. Matsumoto et al., 1997; Sone et al., 2006). Given the low density of weather stations and their limited temporal coverage, characterising the region's climate is difficult, but in general, winter conditions are dominated by the Siberian High pressure system, which develops to the NW, and summer conditions are dominated by the Pacific High, which develops to the SE (Shahgedanova et al., 2002; Yanase and Abe-Ouchi, 2007). These conditions generally result in strong SE to NW climatic gradients, as warm, moist air masses from the North Pacific (the region's principal moisture-source) are driven north and west across the peninsula; whilst cold, continental air masses advance south and east from the continental interior of Siberia. These climatic gradients are evident from climate averages for the 1960-1990 period (from www.climate-charts.com), with mean annual temperature ranging from 1.6 °C in the SE sector of the peninsula to -3.2 °C in the NW; whilst mean annual precipitation ranges from 996 mm $yr^{-1}$ in the SE sector to 478.5 mm $yr^{-1}$ in the NW. These regional variations in temperature and precipitation are also evident in, ~1 km resolution, regional climate grids of the region (see figures 3a and 3b), produced through interpolation between weather station data (see Hijmans et al., 2005), and in mean maximum annual snow depth data for the 1961-1990 period (from Matsumoto et al., 1997) (see figure 3c). Though the low density of available weather stations, and the mountainous nature of much of the peninsula, partly limit the utility of these grids, they are of use in demonstrating the contrast between the western slopes of the Northern Sredinny Mountains, where mean annual temperatures approach -26 °C, but where snowfall is minimal; and the eastern sector of the Eastern Volcanic Plateau, where mean annual temperatures are close to or above 0 °C, but where maximum annual snow depth approaches 2 m.

The peninsula is currently occupied by ~446 small glaciers (Solomina et al., 2007), and their distribution is governed by peak altitudes and moisture-availability (from both the North Pacific and Sea of Okhotsk). Extensive glaciers occupied the peninsula at various periods during the Late Quaternary, and at times extended off-shore to terminate in the

North Pacific and Sea of Okhotsk, though the timing of these events remains uncertain (see Bigg et al., 2008; Nürnberg et al., 2011; Barr and Clark, 2011, 2012b). Palaeoclimatic conditions during these former periods of glaciation are unclear, though model simulations indicate that precipitation over the peninsula was likely reduced at the global Last Glacial Maximum (gLGM; 21 ka)(Yanase and Abe-Ouchi, 2007, 2010; Krinner et al., 2011), when large ice sheets occupied much of North America, and Northern Europe. During the gLGM, no ice sheets occupied NE Russia, but it is apparent that glaciers upon the Kamchatka peninsula extended up to 80 km beyond their current margins. This glacial expansion likely resulted from a reduction in air temperatures relative to present (see Barr and Clark, 2011), but a corresponding decrease in precipitation likely precluded the development of larger ice masses (as found at similar latitudes elsewhere in the Northern Hemisphere at the gLGM).

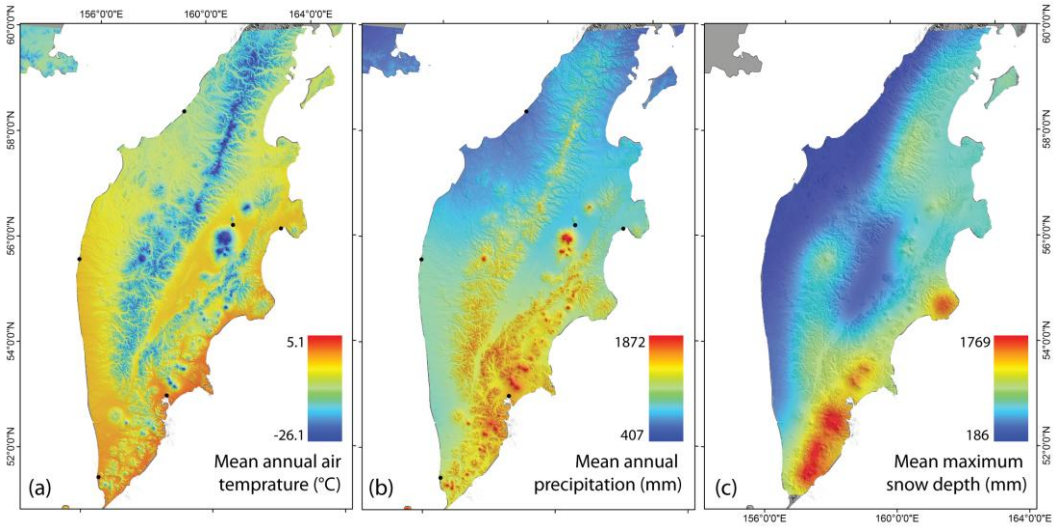


*Figure 3. Generalised depictions of modern climatic conditions across the Kamchatka Peninsula. (a) Mean annual air temperature, and (b) mean annual precipitation for the 1950-2000 period. These data are regional climate grids produced through interpolation between weather station data (see Hijmans et al., 2005)—weather stations are shown as black dots. (c) Mean annual-maximum snow depth grid, for the 1961-1990 period, produced through interpolation of data presented by Matsumoto et al. (1997). [This figure is to be reproduced in colour on the Web (free of charge) and in black-and-white in print]*

## 4. Data and Methods

Cirques were defined according to Evans and Cox (1974), and mapped from Landsat ETM+ satellite images (with a spatial resolution of 15 m), and ASTER GDEM data (with a spatial resolution of 30 m, and an absolute vertical accuracy of ~17 m; ASTER GDEM Validation Team, 2011). Cirques were identified as large, shallow or overdeepened surfaces, enclosed by rather arcuate headwalls, and occupying valley-head settings within high-altitude sectors of drainage basins. Their upper boundaries were often identifiable as a break-of-slope in the DEM, and were drawn to correspond with crest limits (see Federici and Spagnolo, 2004). Lower boundaries were more difficult to define, and were marked either by a transition from shallow cirque floors to steeper slopes down-valley, referred to as the cirque 'threshold' (see figure 4), or by connecting the downstream spurs of arcuate headwalls. Cirques were digitised (in a GIS) as enclosed polygons, allowing morphometric attributes to be readily calculated. Field–based checking (ground-truthing) was not performed, for logistic reasons, and we are aware of no published cirque maps for this region, against which to validate the mapping performed here.

In order to analyse variability in morphometry and azimuth, a number of attributes were recorded for each cirque. Many have been considered in previous investigations, and are defined in detail elsewhere (see: Evans and Cox, 1995; Federici and Spagnolo, 2004). For each cirque, **area (A)** was automatically calculated in a GIS. **Cirque length (L)** was then measured along a straight line connecting the midpoint of the cirque 'threshold' to the cirque headwall, splitting the cirque into two equal halves (see figure 4c). This central line, known as the median axis, was delineated using an automated GIS technique, developed by Federici and Spagnolo (2004). **Cirque width (W)** was measured as the longest line perpendicular to the median axis (see figure 4c), and, again, was calculated using an automated GIS technique developed by Federici and Spagnolo (2004). **Cirque azimuth (Az)** was measured as the orientation of the median axis, and mean vector direction and vector strength were calculated for cirque populations (see Evans, 1977; 2006b). The **minimum ($Alt_{min}$), mean ($Alt_{mean}$) and maximum ($Alt_{max}$) altitude** of each cirque was calculated from the ASTER GDEM data. **Cirque altitudinal range (H)** was recorded as the height difference between $Alt_{min}$ and $Alt_{max}$, and cirque size was

calculated as the cube-root of L*W*H (see Evans, 2006a). The **Mean slope gradient ($S_{mean}$)** of each cirque was automatically calculated in a GIS, and **circularity (circ.)** was measured as the ratio between the perimeter of a cirque and the perimeter of a circle with the same area (see Aniya and Welch, 1981). Ratios between spatial attributes (L/H, W/H, L/W) were analysed, and the generalised geology of each cirque was considered (based upon maps by Persits et al., 1997; and Avdeiko et al., 2007). Finally, the **annual solar insolation ($Sol_{mean}$)** received by each cirque was modelled using the ArcGIS Solar Radiation tool, with summer (June, July, August) and winter (December, January, February) insolation recorded separately. These values are based upon estimates of both direct and diffuse radiation (but not reflected radiation), and account for site latitude, elevation, surface-slope, surface-aspect, and shading from surrounding topography (see Fu and Rich, 2002). Though calculations include estimates of diffuse radiation, they do not explicitly consider the impact of cloud-cover, either in terms of total values or daily and seasonal variations; and the values presented here are therefore regarded as maximum estimates. This is not considered a major limitation, as, for the purposes of this investigation, exact insolation is less important than relative values between cirques.

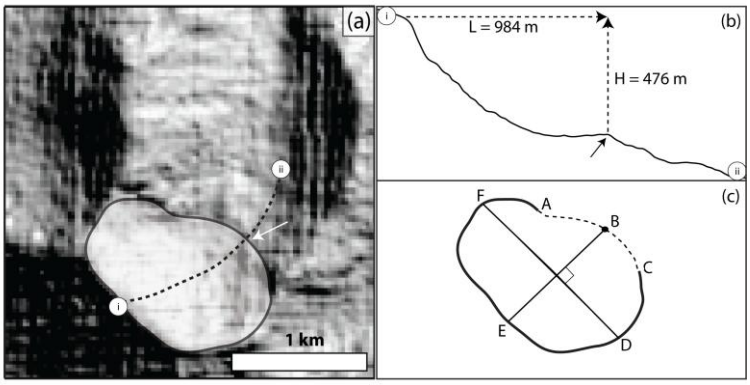


*Figure 4. Example cirque in the Southern Sredinny Mountains (54.17°N, 157.56°E). (a) A shaded-relief image of the ASTER GDEM. The mapped cirque is shown as a semi-transparent (white) polygon. (b) Topographic profile, from 'i' to 'ii', following the dashed line in figure (a), showing the correspondence between the cirque threshold and a step-like transition in topography, from a shallow cirque floor to a steeper slope down-valley (marked as a solid arrow in figures (a) and (b)). L and H are cirque length and altitudinal range, respectively. (c) Definition of spatial attributes: line A-C is the cirque threshold; B is the threshold mid-point; B-E is the median axis (used to define cirque length); D-F is the cirque width (perpendicular to B-E).*

## 5. Results

A total of 3,758 cirques were mapped across the Kamchatka Peninsula, with the majority found within the Sredinny (n = 2,853) and Vostočny (n = 832) Mountains (see figure 2). Approximately 11% (n = 405) are occupied by lakes, and ~6% (n = 238) are occupied by glaciers (glaciers which do not occupy cirques are found upon the slopes of the region's volcanoes). These latter examples effectively represent cirque glaciers and are therefore excluded from the analysis below which will focus on a total population of 3,520 cirques.

### 5.1. Cirque shape

Statistics for cirque attributes are presented in table 2, and demonstrate that cirque length ranges from 125 m to 2,110 m; cirque width ranges from 250 m to 2,601 m; whilst cirque area ranges from 0.031 $km^2$ to 4.017 $km^2$. These dimensions are comparable to cirques found in other regions globally (see table 1). The shortest cirque is found on the west-central slopes of the Sredinny Mountains, where the narrowest and smallest cirques are also found (see figure 5). The longest and widest cirque is found on the NW slopes of the north-central Sredinny Mountains, roughly 250 km north of the shortest cirque (see figure 5). Cirque width and length frequency distributions are unimodal, with slight positive skew, and mean cirque width is greater than length (see figure 6). Correlations between cirque size attributes are strong (see table 3) ($0.70<r<0.93$), and cirques are highly circular (circularity ranges from 1.004 to 1.292), indicating that headwall retreat has occurred in conjunction with cirque widening. Allometric coefficients for L, W and H were calculated for the entire cirque population, using the technique employed by Evans (2006a)—a development of Olyphant (1981). Coefficients were calculated by plotting L, W, and H against cirque size ($\sqrt[3]{LWH}$), and recording the power exponents for each attribute (see figure 7). These exponents were calculated to be 1.00, 1.04, and 0.96 for L, W and H, respectively (see Evans, 2006a, for details about this technique), and indicate that during development, cirques have grown rather isometrically, though widening has slightly outpaced lengthening, which, in turn, has slightly outpaced deepening.

*Table 2. Statistics for analysed cirque attributes**

| | A | L | W | H | Size | $Alt_{min}$ | $Alt_{mean}$ | $Alt_{max}$ | $S_{mean}$ | Circ. | $Sol_{mean}$ | L/H | W/H | L/W |
|---|---|---|---|---|---|---|---|---|---|---|---|---|---|---|
| Min | 0.031 | 125 | 250 | 60 | 133 | 122 | 298 | 508 | 13.38 | 1.004 | 477.62 | 0.92 | 1.02 | 0.50 |
| Mean | 0.730 | 868 | 992 | 421 | 706 | 988 | 1177 | 1408 | 28.10 | 1.054 | 755.08 | 2.12 | 2.43 | 0.90 |
| Max | 4.017 | 2110 | 2601 | 983 | 1556 | 1919 | 2238 | 2543 | 41.97 | 1.292 | 1147.93 | 5.41 | 7.43 | 2.04 |
| Sdev | 0.414 | 247 | 307 | 116 | 179 | 274 | 281 | 301 | 3.71 | 0.037 | 111.76 | 0.53 | 0.67 | 0.21 |
| Skew | 1.76 | 0.70 | 0.80 | 0.34 | 0.47 | -0.61 | -0.58 | -0.42 | -0.10 | 1.520 | 0.59 | 1.20 | 1.14 | 0.75 |
| $10^{th}$ percentile | 0.322 | 587 | 638 | 279 | 497 | 600 | 780 | 996 | 23.41 | 1.017 | 627.87 | 1.54 | 1.66 | 0.66 |
| $90^{th}$ percentile | 1.261 | 1186 | 1400 | 572 | 939 | 1298 | 1492 | 1757 | 32.82 | 1.104 | 922.11 | 2.79 | 3.26 | 1.18 |

*A, area ($km^2$); L, length (m); W, width (m); H, altitudinal range (m); Size, $\sqrt[3]{LWH}$ (m); $Alt_{min}$, $Alt_{mean}$, $Alt_{max}$, minimum, mean, maximum altitude (m.a.s.l.); $S_{mean}$, mean slope gradient (°); Circ., circularity; $Sol_{mean}$, mean annual insolation ($kWh/m^2$).

*Table 3. Pearson product moment correlation among analysed attributes**

| | A | L | W | H | Size | $Alt_{min}$ | $Alt_{mean}$ | $Alt_{max}$ | $S_{mean}$ | Circ. | $Sol_{mean}$ | L/H | W/H | L/W |
|---|---|---|---|---|---|---|---|---|---|---|---|---|---|---|
| A | 1.00 | 0.88 | 0.92 | 0.63 | 0.93 | -0.14 | -0.03 | 0.12 | -0.21 | 0.12 | 0.10 | 0.26 | 0.33 | -0.13 |
| L | | 1.00 | 0.71 | 0.64 | 0.89 | -0.11 | -0.01 | 0.15 | -0.22 | -0.03 | 0.13 | 0.40 | 0.11 | 0.27 |
| W | | | 1.00 | 0.60 | 0.89 | -0.16 | -0.06 | 0.08 | -0.16 | 0.19 | 0.06 | 0.13 | 0.47 | -0.44 |
| H | | | | 1.00 | 0.84 | 0.03 | 0.20 | 0.31 | 0.44 | 0.15 | -0.11 | -0.40 | -0.38 | 0.01 |
| Size | | | | | 1.00 | -0.09 | 0.05 | 0.24 | 0.02 | 0.11 | 0.03 | 0.05 | 0.09 | -0.08 |
| $Alt_{min}$ | | | | | | 1.00 | 0.98 | 0.92 | 0.18 | 0.08 | 0.33 | -0.16 | -0.21 | 0.09 |
| $Alt_{mean}$ | | | | | | | 1.00 | 0.97 | 0.27 | 0.10 | 0.31 | -0.24 | -0.27 | 0.08 |
| $Alt_{max}$ | | | | | | | | 1.00 | 0.33 | 0.13 | 0.26 | -0.30 | -0.34 | 0.08 |
| $S_{mean}$ | | | | | | | | | 1.00 | 0.05 | -0.32 | -0.79 | -0.67 | -0.06 |
| Circ. | | | | | | | | | | 1.00 | -0.02 | -0.19 | 0.07 | -0.21 |
| $Sol_{mean}$ | | | | | | | | | | | 1.00 | 0.29 | 0.19 | 0.08 |
| L/H | | | | | | | | | | | | 1.00 | 0.63 | 0.30 |
| W/H | | | | | | | | | | | | | 1.00 | -0.51 |
| L/W | | | | | | | | | | | | | | 1.00 |
| HI | | | | | | | | | | | | | | |

*See table 2 for definition of attributes*

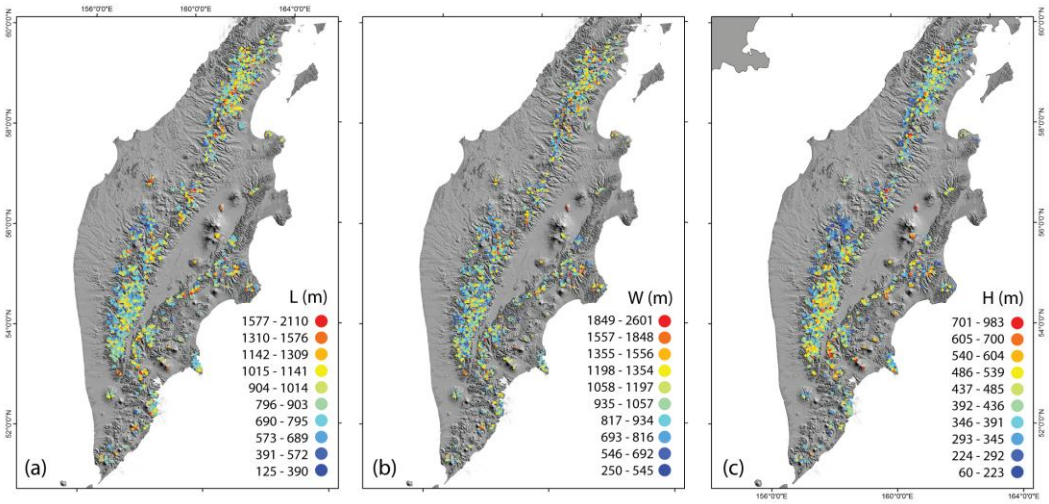


*Figure 5. Spatial distribution of (a) cirque length, L; (b) width, W; and (c) altitudinal range, H. [This figure is to be reproduced in colour on the Web (free of charge) and in black-and-white in print]*

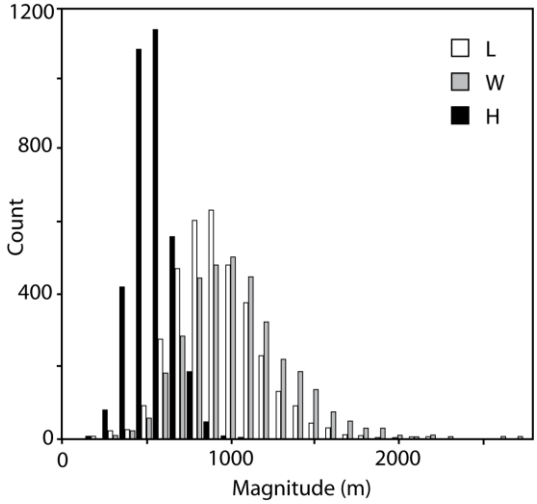


*Figure 6. Frequency distributions for cirque length (L), width (W) and altitudinal range (H).*

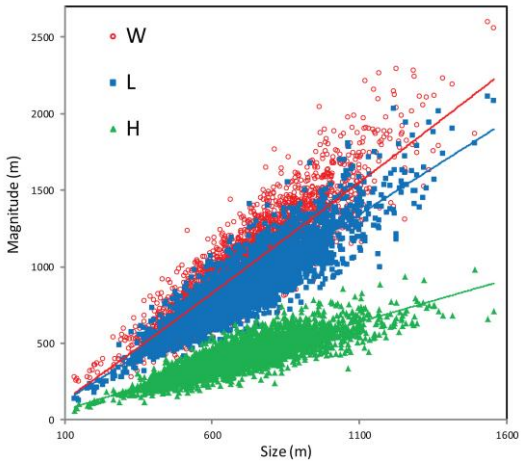


*Figure 7. Cirque length (L), width (W), and altitudinal range (H), plotted against cirque size ($\sqrt[3]{LWH}$). L, exponent = 1.00, $r^2$ = 0.82; W, exponent = 1.04, $r^2$ = 0.79; H, exponent = 0.96 $r^2$ = 0.75.*
*[This figure is to be reproduced in colour on the Web (free of charge) and in black-and-white in print]*

### 5.2. Cirque Azimuth

When the azimuths of all 3,520 cirques are considered, it is apparent that they show a very strong N bias (see figure 8a). The vector mean for the entire dataset is 006°, with a vector strength (which highlights the extent of deviation from a uniform distribution with aspect) of 46% (see Evans, 1977). In total, 26% of cirques are found to be N-facing (337.5-22.5° interval), with the highest frequency peak covering the 350–360° interval (see figure 8a). Other, less distinct, azimuthal peaks are found at 20–30° (NE), and 310–320° (NW). Very few cirques are S-facing, with only 3% occupying the 157.5–202.5° (S) interval (see table 4). This N bias in cirque azimuth is highlighted by the fact that there is no corresponding asymmetry in the orientation of the region's mountain slopes (e.g. ~12.7% of slopes are north-facing, and 12.9% are south-facing)(see table 4).

When cirque populations within each of the region's principal mountain chains (the Northern Sredinny Mountains, Southern Sredinny Mountains, Vostočny Mountains, and Eastern Volcanic Plateau; see figure 2 for mountain range locations) are considered independently, there appears to be little inter-regional variability in azimuth vector means (see figure 8b-e). However, rose diagrams for the Vostočny Mountains and Eastern Volcanic Plateau show bimodal distributions (see figure 8d and 8e), with cirques in the Vostočny Mountains having frequency peaks in the 10–20° and 350–360° intervals (figure 8d), and cirques upon the Eastern Volcanic Plateau having frequency peaks in the 40–50° and 350–360° intervals (figure 8e). There is also inter-regional variability in vector strength, ranging from 36% in the Vostočny Mountains, 44% in the Northern Sredinny, 50% in the Southern Sredinny, to 61% upon the Eastern Volcanic Plateau. Part of this variability in vector strength may relate to inter-regional variations in cirque number (e.g. ranging from 1,841 cirques in the Southern Sredinny Mountains to 177 upon the Eastern Volcanic Plateau).

*Table 4. Distribution of cirque attributes* with aspect*

| | N | NE | E | SE | S | SW | W | NW |
|---|---|---|---|---|---|---|---|---|
| Number of cirques | 912 | 793 | 393 | 166 | 103 | 164 | 362 | 627 |
| A | 0.71 | 0.72 | 0.72 | 0.87 | 0.91 | 0.75 | 0.71 | 0.72 |
| L | 832 | 866 | 886 | 961 | 959 | 878 | 872 | 869 |
| W | 1005 | 982 | 954 | 1071 | 1116 | 1023 | 956 | 982 |
| H | 408 | 425 | 436 | 443 | 437 | 407 | 416 | 421 |
| Size | 686 | 706 | 710 | 762 | 769 | 708 | 696 | 704 |
| $Alt_{min}$ | 936 | 975 | 1045 | 1092 | 1074 | 1042 | 1034 | 959 |
| $Alt_{mean}$ | 1118 | 1168 | 1245 | 1293 | 1271 | 1224 | 1225 | 1146 |
| $Alt_{max}$ | 1345 | 1400 | 1481 | 1535 | 1511 | 1449 | 1451 | 1379 |
| $S_{mean}$ | 28.10 | 28.11 | 28.72 | 27.48 | 27.08 | 27.01 | 28.14 | 28.29 |
| Circ. | 1.05 | 1.06 | 1.06 | 1.06 | 1.05 | 1.05 | 1.05 | 1.05 |
| $Sol_{mean}$ | 670.87 | 706.60 | 821.15 | 940.34 | 981.31 | 937.17 | 830.19 | 720.35 |
| L/H | 2.10 | 2.09 | 2.08 | 2.25 | 2.27 | 2.26 | 2.16 | 2.12 |
| W/H | 2.54 | 2.37 | 2.24 | 2.50 | 2.66 | 2.63 | 2.36 | 2.40 |
| L/W | 0.86 | 0.91 | 0.95 | 0.92 | 0.87 | 0.88 | 0.95 | 0.91 |
| Land-surface (%)† | 12.7 | 13.1 | 12.9 | 11.4 | 12.9 | 13.0 | 12.8 | 11.2 |

* N, 337.5-22.5°; NE, 22.5-67.5°; E, 67.5-112.5°; SE, 112.5-157.5°; S, 157.5-202.5°; SW, 202.5-247.5°; W, 247.5-292.5°; NW, 292.5-337.5.†Land surface reflects the percentage of mountain topography within each azimuth class. See table 2 for further definition of attributes.

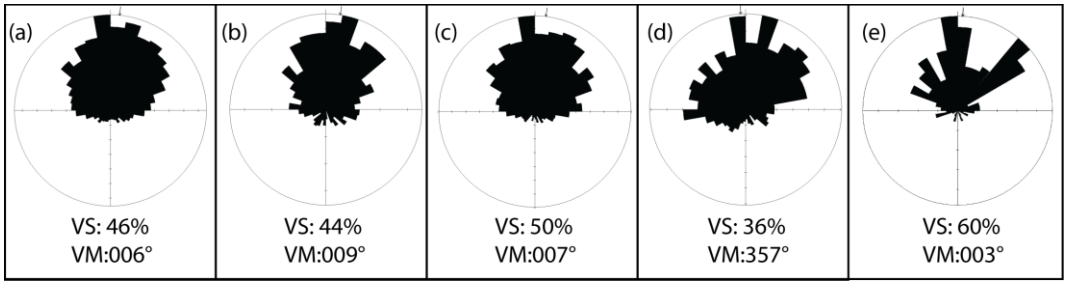


*Figure 8. Rose diagrams of cirque aspect frequency. For (a) all cirques (n = 3,520); (b) the Northern Sredinny Mountains (n = 846); (c) the Southern Sredinny Mountains (n = 1,841); (d) the Vostočny Mountains (n = 656); and (e) the Eastern Volcanic Plateau (n = 177). The vector strength (VS) and Vector Mean (VM) are also shown (the arrow in each diagram corresponds to the vector mean). See figure 2 for mountain range locations.*

### 5.3. Altitudinal parameters

The minimum altitude of individual cirques ranges from 122 m (a.s.l.) to 1,919 m. Their mean altitude ranges from 298 m (a.s.l.) to 2,238 m (a.s.l.); whilst their maximum altitude ranges from 508 m (a.s.l.) to 2,543 m (a.s.l.)(see table 2). These three altitudinal variables are strongly correlated ($0.92<r<0.99$), but are weakly correlated with other attributes (see table 3). Cirque altitude varies with aspect, as SE-facing cirques are highest ($Alt_{min}$, $Alt_{mean}$ and $Alt_{max}$) and N-facing cirques are lowest (see table 4). Cirque altitudinal range (H) varies between 60 m, and 983 m, and shows a unimodal frequency distribution (see figure 6). Cirques exhibiting the lowest altitudinal range are found upon the west-central slopes of the Sredinny Mountains (see figure 5), whilst those with the highest are found upon the flanks of some of the region's volcanoes. Altitudinal range also varies with altitude ($r \leq 0.31$), whereas cirque length and width do not (see Table 3).

### 5.4. L/H, W/H and L/W ratios

L/H ranges from 0.92 to 5.41. W/H ranges from 1.02 to 7.43; whilst L/W ranges from 0.50 to 2.04. L/H vales are highest for S, SE and SW-facing cirques and lowest for those facing E, NE and N (see table 4), though S-facing cirques are longer, wider and deeper than those facing N (see table 4). W/H and L/W show little variation with cirque aspect, and show little correlation with other attributes (see table 3).

### 5.5. Cirque slope gradients

Mean cirque slope gradient varies from 13° to 42°. Lower values are found for S, SW, and SE-facing cirques, and these slopes also harbour the largest cirques (see table 4). There is no strong relationship between slope gradient and other attributes, though cirque slope generally increases with altitude ($r \leq 0.33$), and altitudinal range ($r = 0.44$)(see table 3).

### 5.6. Cirque insolation

Modelled annual insolation per cirque varies from 478 kWh/m$^2$ to 1,173 kWh/m$^2$ (see table 2). There is little correlation between mean annual insolation and cirque dimensions (see table 3), but (unsurprisingly) insolation shows a clear relation to aspect (see figure 9a). This relationship is stronger when winter (Dec, Jan, Feb) insolation alone is considered (figure

9b), and weaker when summer (June, July, August) insolation is considered (figure 9c). There is an increase in insolation with cirque altitude, though this relationship is not strong ($r \leq 0.33$)(see table 3), while there is no clear relationship between cirque insolation and latitude ($r = 0.06$).

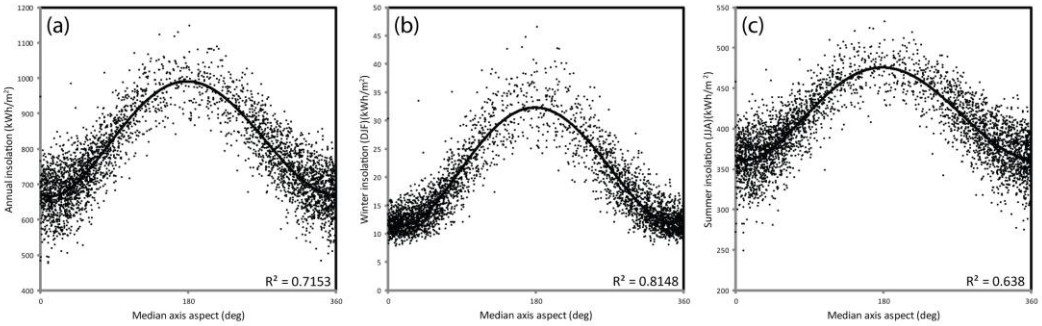


*Figure 9. Modelled mean insolation per cirque plotted against median axis azimuth. (a) Annual insolation; (b) Winter insolation (Dec, Jan, Feb); (c) Summer insolation (June, July, August). In each figure, a fourth-order polynomial trend line is also plotted (upon which the $R^2$ values are based).*

### 5.7. Geology

The region's generalised geology is here considered (based upon Persits et al., 1997; and Avdeiko et al., 2007). Eight units are distinguished: with 18% of Kamchatkan cirques found upon metamorphic complexes; 8% upon collision granitoids; 3% upon Cretaceous terrigenous deposits; 16% upon Upper Cretaceous and Paleocene volcanic and volcanic-terrigenous deposits; 3% upon Cretaceous-Eocene island-arc units; 1% upon Paleocene-Miocene deposits; 32% upon Miocene-Pliocene volcanic complexes; and 19% upon Quaternary volcanic complexes. For a number of cirque attributes, a one-way analysis of variance (ANOVA) is used to estimate the variability accounted for by the 8 geological classes (based upon the approach of Evans, 2006a). Results are shown in table 5 and figure 10, and indicate that the attribute most closely related to geology is cirque floor altitude (figure 10a). Much of this relationship appears to be governed by one geological unit (Cretaceous-Eocene island-arc units), where cirques have altitudes noticeably lower than within other groups (figure 10a). Initially, this might suggest some geological control upon cirque altitude; however, it is apparent that, when considered across the peninsula, this geological unit is predominantly found at low altitude sites (see figure 11). Therefore, the correspondence with cirque altitude likely reflects this geographical distribution, rather than a geological control. There appears to be some correspondence between geology and cirque slope gradient, L/H, and W/H (table 5) though the data show no clear trends between different units (figure 10b and c). Cirque size attributes (L and W) show very little relation to geology (see figure 10d)—something also found for cirques in other parts of the world (e.g. Evans, 2006a).

*Table 5. Analysis of variance (ANOVA) results relating cirque attributes to bedrock geology (geological units outlined in figure 10).*

| | $R^2$ (adjusted) | F-ratio | P-value |
|---|---|---|---|
| $Alt_{min}$ | 0.216 | 139.8 | 0.0000 |
| $S_{mean}$ | 0.188 | 118.0 | 0.0000 |
| L/H | 0.091 | 51.8 | 0.0000 |
| W/H | 0.085 | 47.9 | 0.0000 |
| H | 0.033 | 18.4 | 0.0000 |
| Circ. | 0.018 | 10.5 | 0.0000 |
| W | 0.009 | 5.8 | 0.0000 |
| L | 0.009 | 5.9 | 0.0000 |
| L/W | 0.001 | 0.8 | 0.5814 |

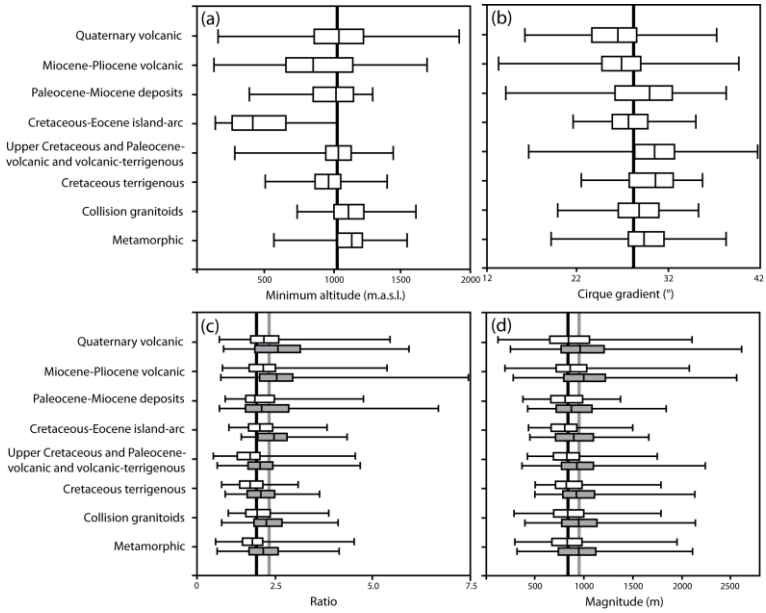


*Figure 10. Box plots depicting variation in cirque attributes with geology. In each figure, the box represents the inter-quartile range, the 'whiskers' reflect the total data range, and vertical lines reflect the sample medians (where contained within the inter-quartile box) and population medians. (a) Variation in minimum cirque altitude. (b) Variation in cirque gradient (mean). (c) Variation in L/H (white box-plot and black population median) and W/H (grey box-plot and grey population median). (d) Variation in cirque length (white box-plot and black population median) and width (grey box-plot and grey population median).*

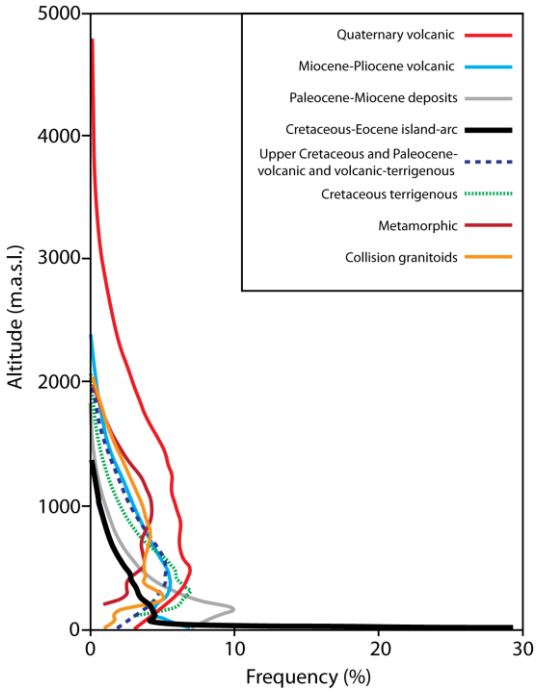


*Figure 11. Elevation frequency distributions for different geological units across the Kamchatka Peninsula. This image demonstrates that Cretaceous-Eocene island-arc units are typically found at low altitude sites, and explains the prevalence of the low-altitude cirques in areas characterised by this bedrock geology. [This figure is to be reproduced in colour on the Web (free of charge) and in black-and-white in print]*

## 6. Discussion

### 6.1. Controls upon cirque azimuth

Across the Kamchatka Peninsula, cirque azimuth is strongly biased towards N, NE, and NW directions—a trend common for many Northern Hemisphere glaciers and cirques (see Evans, 1977, 2006b). The dominance of N-facing cirques likely reflects minimum daily insolation (limiting snow and ice ablation) upon such slopes (see figure 9). Winter insolation shows

a particularly strong relationship with cirque azimuth ($r^2$ = 0.81) (figure 9b), potentially reflecting the intensification of aspect-related variations in insolation during winter months (when sun angles are lowest). The slight NE deflection of azimuth vector mean identified in this study (see figure 8a) likely reflects diurnal variations in temperature, as NE-facing slopes receive much of their direct solar radiation in the morning, when temperatures are relatively low (see Evans, 1977, 2006b). The peak in the frequency of NNW-facing cirques (see figure 8a) likely reflects glacier growth (and associated cirque development) in lee of snow-bearing winds from the North Pacific (to the SSE), and is a trend common to modern glaciers upon the peninsula, which have a vector mean aspect of 334° (Evans, 2006b). When the entire cirque population is considered (n = 3,520), there is limited evidence for structural (non-climatic) control upon azimuth. This is reflected in the lowest row of table 4, where the total land surface area in each azimuth class is listed, demonstrating that the tendency for cirques to preferentially occupy N-facing slopes is not controlled by structure. This apparent lack of structural-control may reflect the fact that such influences are often unobserved when large areas and/or large cirque populations are considered (see Evans, 2006b). This assertion is supported, to some degree, by inter-regional differences in cirque aspect. For example, cirques of the Vostočny Mountains show a tendency towards NW aspects (when compared to the total population), and cirques of the Eastern Volcanic Plateau show a greater tendency towards NE aspects (see figures 8d and 8e, respectively). The Vostočny Range has a general NE-SW orientation (~14% of the region's slopes are W-facing), likely favouring cirque development upon NW slopes, and the Eastern Volcanic Plateau has a general NW-SE orientation (~14.3% of slopes are E-facing), likely favouring cirque development upon NE slopes. Thus, structural control upon cirque azimuth is potentially identifiable when the region's mountain chains are considered independently.

### 6.2. Palaeoglacial significance of the cirque record

From the perspective of cirque development, mountain glaciation might be classified into three phases (depicted in figure 12). **Phase 1:** An active phase, during the initial stages of glaciation, when glaciers are small and erode the cirques to which they are confined. This erosion is driven by the coincidence of equilibrium-line altitudes (ELAs) and cirque altitudes (see figure 12a). **Phase 2:** A passive phase, when cirque-erosion is minimal, as glaciers grow to form valley glaciers (and other larger ice masses). In such circumstances, erosion is again concentrated at ELAs, which now lie below cirque altitudes. Cirques are found within glacial accumulation zones, and are likely occupied by cold based, minimally-erosive ice (see figure 12b). **Phase 3:** An active phase, when, during retreat, glaciers return to the confines of their cirques, where they actively-erode, before finally disappearing (see figure 12c). Given these relationships, the morphometry of cirques upon the Kamchatka Peninsula is here considered with reference to these three phases (see figure 12).

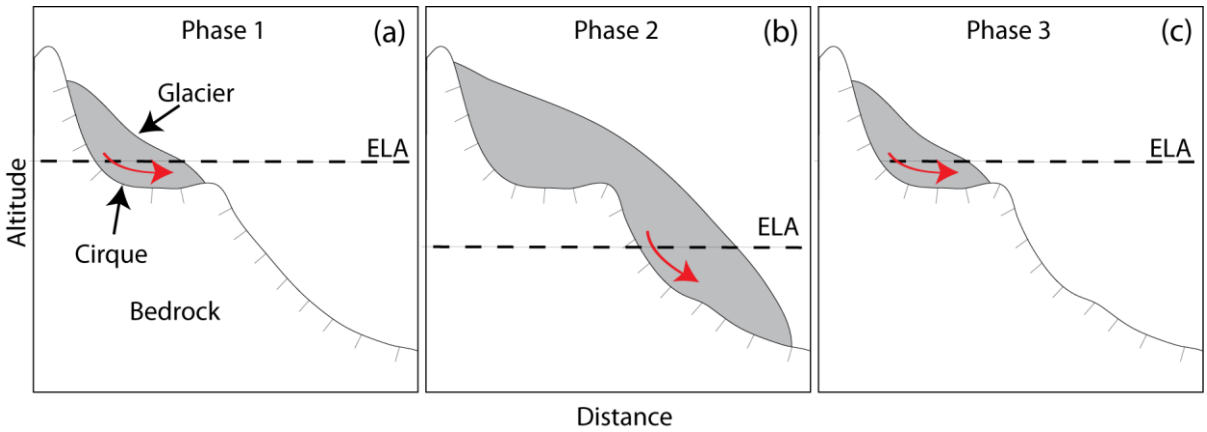


*Figure 12. Schematic illustration of a three phases of mountain glaciation and their relation to cirque erosion. (a) Phase 1: during the initial stages of glaciation, glaciers are small and readily erode the cirques to which they are confined. (b) Phase 2: glaciers advance beyond the confines of the cirque, and focus erosion at lower altitudes. Under such circumstances, cirques are likely occupied by cold based, minimally-erosive ice. (c) Phase 3: during retreat, glaciers return to the confines of their cirques, where they might actively-erode, before finally disappearing. In each figure, the site of greatest glacial erosion is depicted by a red arrow, and coincides with the equilibrium-line altitude (ELA), where rotational flow is maximised.*

#### 6.2.1. Cirque Isometry

L/W ratios (with a mean value of 0.90) indicate that cirques upon the Kamchatka Peninsula are naturally circular in shape (with a mean circularity of 1.054). This applies to small and large cirques alike, suggesting that this shape develops even during the early stages of growth—as noted by Federici and Spagnolo (2004) in the European Alps. Volumetric analysis

(based upon Olyphant, 1981; Evans, 2006a) suggests that cirques have developed rather isometrically (growing equally in all dimensions), though widening has slightly outpaced lengthening, which in turn has slightly outpaced deepening (i.e. coefficients for L, W and H, are 1.0003, 1.0378, and 0.9619, respectively). The coincidence of widening, lengthening and deepening is common to cirques globally (see Evans and Cox, 1995; Evans and McClean, 1995; Federici and Spagnolo, 2004; Evans, 2006a), but, development is often found to be allometric—with cirque deepening *clearly* outpaced by lengthening and widening (the coefficient for H typically lies between 0.66 and 0.91). Here we consider two hypotheses to explain the isometric record found in the present study. **Hypothesis 1:** the absence of an allometric record of cirque development upon the peninsula reflects the region's size, varied structure and lithology (Evans, 1994; Sauchyn et al., 1998; Hughes et al., 2007), combined with the large number of cirques considered. This assertion is supported, to some degree, by Evans (2006a) who suggests that heterogeneity in geological structure and lithology might explain the limited evidence of allometric cirque development in the mountains of Wales (coefficient for H = 0.91). **Hypothesis 2:** Cirque-type glaciers (phases 1 and 3, figure 12a and figure 12c) 'naturally' produce isometric cirques, but are rarely afforded time to do so, because they quickly grow to form valley glaciers and larger ice masses (phase 2, figure 12b). The suggestion is that this growth effectively terminates (or at least suppresses) the process of cirque deepening, but allows lateral erosion (increasing L and W) to partly continue, as a result of both glacial and periglacial processes (see Sanders et al., 2012a). Thus, cirques begin to develop an allometric form, as lengthening and widening outpace deepening. Given this hypothesis, the apparent isometry of cirques upon the Kamchatka Peninsula might suggest that cirque-type glaciation (phases 1 and 3) has dominated, with glaciers rarely extending beyond their cirque settings (i.e. rarely entering phase 2). Despite this suggestion, the premise upon which this hypothesis is based, i.e. that cirque glaciers 'naturally' result in isometry, remains untested, and it might equally be hypothesised that cirques glaciers 'naturally' result in allometry, and that the growth of valley glaciers (phase 2) enhances deepening relative to both lengthening and widening (resulting in isometry). However, this suggestion is more difficult to reconcile with figure 12, as it is unclear what mechanism would lead to an increase in cirque deepening, relative to lengthening and widening, upon moving from cirque-type to valley-type glaciation—particularly as rotational flow within cirques is likely to diminish under such conditions (see figure 12). In fact, recent evidence supports the notion that erosion of cirque headwalls operate at rates roughly equivalent to vertical incision (see Sanders et al., 2012b), likely resulting in isometric development.

### 6.2.2. Cirque size

Cirque size (including L, W and H) varies as a function of aspect (see table 4 and figure 13a), with largest cirques (L, W and H) found upon S and SE-facing slopes (see table 4). The horizontal dimensions of cirques are considered governed by glacial erosion, freeze-thaw processes, and possibly geology (McCall, 1960), whilst cirque deepening is thought to be largely governed by subglacial erosion (see Gordon, 1977). There is little evidence for geological control on cirque dimensions upon the Kamchatka Peninsula (see table 5 and figure 10), thus, large and deep cirques may reflect the intensity of freeze-thaw cycles and/or glacial erosion. There is certainly evidence to support the idea that freeze-thaw cycles are more frequent upon S and SE facing slopes, as daily and annual variations in insolation, and therefore temperature, are maximised (see Federici and Spagnolo, 2004). There is also possible evidence to support the idea that upon the Kamchatka Peninsula, glacial erosion was intensified upon S and SE facing slopes, as former glaciers with these aspects likely lay in pathway of moisture-bearing winds from the North Pacific (i.e. to the S and SE), and were therefore dynamic and erosive as a function of their steep mass balance gradients. Cirque enlargement upon S and SE facing slopes, and elsewhere, may also have been intensified if glaciers in the region were largely of cirque-type (phase 1), rarely extending beyond cirque confines to form valley glaciers (phase 2). The dominance of such cirque-type glaciation would have resulted in extensive erosion of both cirque floors and walls, as rotational flow and resultant erosion would have persisted throughout glacial occupation (see figures 12a and 12c).

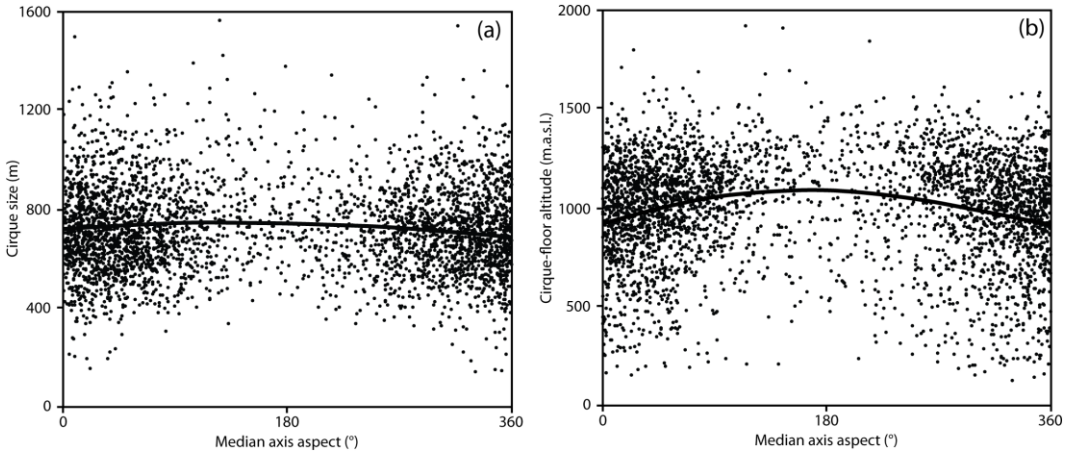


*Figure 13. (a) cirque size, and (b) Cirque floor altitude, plotted against median axis aspect. Also shown are a third-order polynomial trend lines fitted to these data.*

### 6.2.3. L/W classification

The ratio between cirque length and width (L/W) has been used previously to classify cirques according to their history, i.e. whether erosion has been dominated by cirque-type glaciers (phases 1 and 3), valley glaciers (stage 2), or by post-glacial processes (see Damiani and Pannuzi, 1987; Federici and Spagnolo, 2004; Steffanová and Mentlík, 2007). According to this system, ~28% of the cirques upon the Kamchatka Peninsula were formerly occupied by valley glaciers (L/W>1); ~72% were occupied by cirque-type glaciers (0.5<L/W<1), and very few (n = 5) have been highly eroded by post-glacial processes (L/W<0.5). These classifications appear to suggest that, in the past, the peninsula has been occupied by a high proportion of small, cirque-type glaciers (phase 1 and 3), which allowed cirque width to exceed length.

### 6.2.4. The law of decreasing glacial asymmetry with increasing glacier cover

The 'law of decreasing glacial asymmetry with increasing glacier cover' (see Evans, 1977), states that when peaks lie just above regional ELAs (as in phases 1 and 3, figures 12a and 12c), glaciers can only develop (and erode cirques) upon climatically-favourable slopes (NNE-facing, in the case of Kamchatka). Where peaks extend far above the ELA, i.e. where glaciation is extensive (as in phase 2, figure 12b), glaciers can also form upon less-favourable slopes (from a climatic perspective), even at comparatively low altitudes (García-Ruiz et al., 2000; Hughes et al., 2007). Thus, in regions where glaciation has been extensive (phase 2), cirques are found to have a range of azimuths, and lie at a range of altitudes; whereas in regions where glaciation has been 'marginal' (phases 1 and 3), there is a strong bias in cirque azimuths, as examples upon unfavourable slopes are few, and are only found upon the highest mountains. This impact, of former glaciation-extent upon cirque azimuth, is demonstrated in the present study by separating the cirque population (n = 3,520), by altitude, into ten discrete groups of 352. Rose diagrams, showing aspect frequency for each of these groups (see figure 14), demonstrate that, as the altitude of cirque populations increases, vector strength diminishes—reflecting the ability of high mountains to support glaciers with a variety of azimuths. This pattern is repeated when cirque floor altitude is plotted against cirque azimuth (see figure 13b), as SE-facing cirques have highest altitudes ($Alt_{min}$, $Alt_{mean}$ and $Alt_{max}$) whilst those facing N have lowest (see table 4 and figure 13b). These trends, combined with the strength of the N bias in cirque orientation (see section 6.2), would appear to indicate that, upon the Kamchatka Peninsula, former glaciation has often been 'marginal' (phase 1 and 3), characterised by mountain peaks lying just above regional ELAs. This assertion might be partly tested by comparing former ELAs to regional topography to ascertain whether peaks are sufficiently elevated to have supported significant ice masses during former periods of glaciation. Barr and Clark (2011) reconstructed gLGM ELA in the Sredinny Mountains, where Barr and Spagnolo (under review) also analyse cirque altitudes (based on the dataset presented here), as a proxy for mean Quaternary ELA. These data indicate that a significant area of land is found above cirque floor altitudes and gLGM ELAs, with peak altitudes on average found to exceed cirque-floor altitudes and gLGM ELAs by 747 and 849 m, respectively (see Barr and Spagnolo, in prep). This significant area of land above regional ELAs appears not to support the idea that former glaciation in the Sredinny Mountains was marginal, and in fact suggests glaciation comparable to phase 2. There is also geomorphological and offshore evidence to suggest that the entire Kamchatka Peninsula was, in fact, extensively glaciated at periods during the Late Quaternary (see Bigg et al., 2008; Nürnberg et al., 2011; Barr and Clark, 2012a,b). If, as these published data would appear to suggest, the peninsula was extensively glaciated at periods, then the evidence of marginal glaciation suggested by the cirque record might indicate that these episodes of extensive glaciation (i.e. phase 2) were short-lived, and separated by long periods of cirque-type glaciation

(phases 1 and 3). This assertion is supported, to some degree, by Barr and Clark (2012b, figure 9) who suggest that during the past 140 ka, periods of extensive ice advance upon the peninsula occurred at ~128-139 ka, ~41-36 ka, and at the gLGM, and were interspersed by periods of limited glaciation (though chronological control remains limited). Following deglaciation from the gLGM it is likely that short-term, millennial-scale phases of ice advance resulted in further modification of cirque morphometry. Evidence for such phases is preserved as a series of moraines within some of the region's cirques (see Savoskul and Zech, 1997).

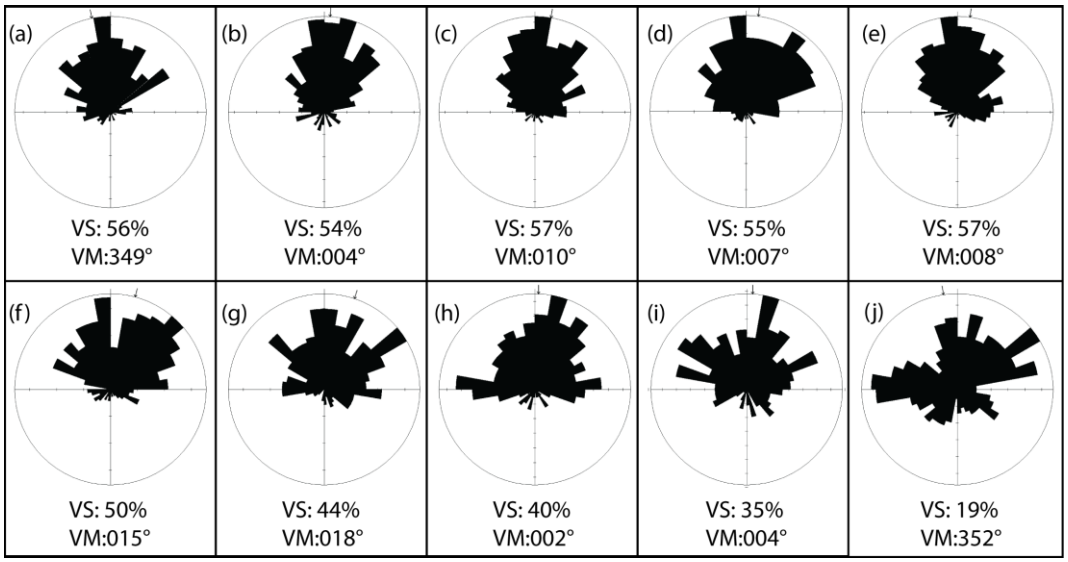


*Figure 14. Rose diagrams showing aspect frequency of cirques grouped according to their minimum altitude (352 cirques are represented in each diagram). Groups range from (a) the lowest 352 cirques, to (j) the highest 352 cirques. The image demonstrates a reduction in vector strength (VS) with altitude. In each image, the arrow corresponds to the Vector Mean (VM).*

### 6.2.5 Summary of palaeoglacial significance of the cirque record

It is evident, based upon the discussion above, that there is no unique way of interpreting the morphometric data obtained within the present study. However, when considered as a whole, the recurring interpretation, which potentially explains all observations (sections 6.2.1 – 6.2.4), is that during the Late Quaternary, glaciation upon the Kamchatka peninsula was marginal, characterised by high ELAs (relative to the topography), and the presence of cirque-type glaciers (phases 1 and 3). Such conditions were likely interspersed with shorter periods of extensive glaciation (characteristic of phase 2), which were less influential in shaping cirque morphology.

## 6.3. Palaeoclimatic significance of the cirque record

The characteristics of marginal glaciation, outlined in section 6.2, likely reflect a climatic restriction to glacier growth upon the Kamchatka Peninsula during much of the Late Quaternary. This certainly appears to be true of the gLGM, when, according to outputs from several general circulation models, moisture availability to the NW Pacific was reduced by the weakening of the North Pacific High during summer months and the intensification of the Aleutian Low during winter (see figure 15) (Yanase and Abe-Ouchi, 2007, 2010)—driven by the expansion of the Laurentide Ice Sheet, and associated increase in albedo, over North America (Yanase and Abe-Ouchi, 2010). This aridity over Kamchatka, and the NW Pacific as a whole, was likely intensified by the expansion of sea ice, a reduction in global sea levels, cooler sea surface temperatures, and the localised growth of glaciers at the gLGM (see Caissie et al., 2010; Yanase and Abe-Ouchi, 2010; Barr and Clark, 2011, 2012b). Given these controls, such aridity may well have been characteristic of much of the Late Quaternary, driven by global cooling, and the growth of ice sheets elsewhere in the Northern Hemisphere. This assertion is potentially supported by some of the cirque azimuth data from the present study, as azimuth-related variations in cirque altitude are considered a proxy for palaeo cloud-cover (Evans, 2006b). This suggestion is founded on the assumption that when cloudy conditions prevail, daily variations in insolation (morning-afternoon) are reduced (Evans, 2006b), and the difference between N and S-facing slopes, in terms of the total insolation they receive, is diminished. This results in a weakening of azimuth-related variations in cirque altitude, as comparatively low-altitude glaciers are able to form, even upon climatically-unfavourable slopes. On this basis, it might be argued that comparatively cloud-free, and therefore arid, conditions prevailed upon the Kamchatka Peninsula during former periods of glaciation, as azimuth-related variations in cirque altitude are clearly apparent (see figure 13b).Thus the cirque record perhaps supports the idea that in the NW

Pacific, despite a reduction in air temperatures, Late Quaternary glaciation was marginal as a result of increased aridity, relative to present. It is probable that regional cooling allowed glaciers to develop upon the peninsula during the last glacial cycle, but that their extent was regulated by the availability of moisture, which was, in turn, governed by the extent of ice sheets elsewhere in the Northern Hemisphere. Thus, glaciation upon the peninsula (and in NE Russia as a whole) may have been out-of-phase with the Laurentide Ice Sheet (see Stauch and Gualtieri, 2008; Krinner et al., 2011; Barr and Clark, 2012b), with short periods of extensive advance perhaps occurring early and/or late during the glacial cycle, when Northern Hemisphere temperatures were reduced, but precipitation was still relatively. Evidence of comparatively restricted ice extent during the gLGM, as a result of extreme aridity, is also found at other sites in central and eastern Asia, including Siberia (Stauch et al., 2007; Stauch and Gualtieri, 2008; Krinner et al., 2011), Tibet (Lehmkuhl and Owen, 2005; Heyman et al., 2011), Japan and Taiwan (Ono et al., 2005; Sawagaki and Aoki, 2011), supporting some of the conclusions presented here. These conditions are in contrast to the NE Pacific (along the western coast on North America), where mean annual precipitation increased significantly at the gLGM (see Kohfeld and Harrison, 2000; Yanase and Abe-Ouchi, 2007, 2010) (see figure 15c and 15f)."

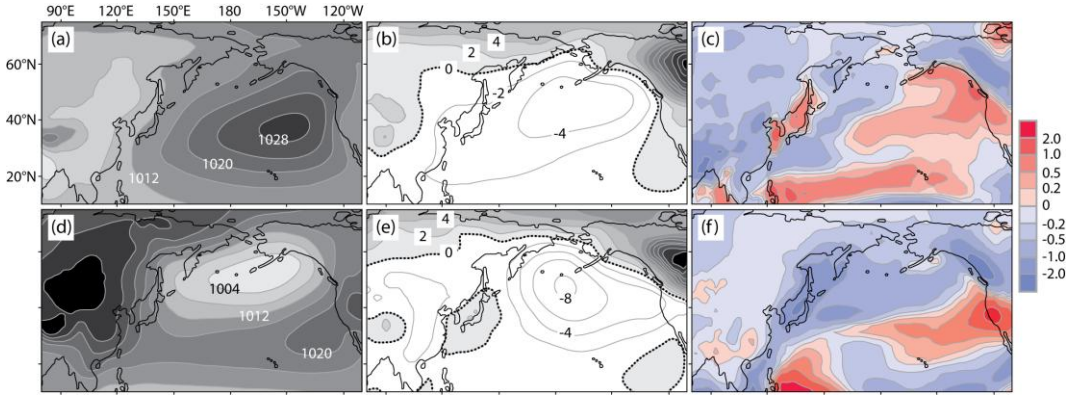


*Figure 15. Sea level pressure (hPa) and precipitation (mm/day) over the North Pacific at the present day and at the global Last Glacial Maximum (gLGM), based upon a summary of outputs from several coupled atmosphere-ocean general circulation models in the PMIP2 database (all figures adapted from Yanase and Abe-Ouchi, 2007). (a) Present-day model mean sea level pressure for June, July and August (JJA). (b) Anomaly (gLGM – present day) for the model mean sea level pressure for JJA. (c) Anomaly (gLGM – present day) for the model mean precipitation for JJA. (d) As (a), but for December, January and February (DJF). (e) As (b), but for DJF. (f) As (c), but for DJF. These outputs suggest that during the gLGM, relative to present, the North Pacific High was weakened during summer months, and that the Aleutian Low was intensified during winter—resulting in a reduction in precipitation over Kamchatka during both summer and winter. This contrasts with increased precipitation along the western coast on North America. [This figure is to be reproduced in colour on the Web (free of charge) and in black-and-white in print]*

## 7. Conclusions

A total of 3,758 cirques have been systematically mapped across the Kamchatka Peninsula, and the properties of 3,520 of these have been analysed (one of the largest cirque populations ever investigated). The main findings of this study can be summarised as follows:

1. Cirques upon the peninsula show a very strong N bias in their azimuth (orientation), with the majority found to face N, NE or NW. This is likely a result of aspect-related variations in insolation (particularly during winter months) and, to a lesser degree, prevailing wind directions.

2. Cirque morphometry appears to suggest that, during the Late Quaternary, conditions upon the Kamchatka Peninsula were characterised by marginal, cirque-type glaciation, with comparatively high ELAs. Factors which potentially support this hypothesis include: evidence for isometric cirque deployment; the fact that ~72% of the region's cirques are characterised as having been occupied by cirque-type glaciers; and the scarcity, altitude, and size of S and SE-facing cirques. Thus, the record suggests marginal glaciation, yet published reconstructions indicate extensive ice-advance at various periods (see Bigg et al., 2008; Nürnberg et al., 2011; Barr and Clark, 2012b). The cirque record is therefore considered to indicate that phases of extensive ice-advance were comparatively short-lived, and that cirque-type glaciers were generally more characteristic of the region.

3. The intensity of azimuth-related variations in cirque altitude, combined with evidence for marginal glaciation (see point 2 above), potentially reflects aridity and comparatively cloudless skies across the peninsula during former periods of glaciation. These conditions were likely governed by negative pressure anomalies over the North Pacific (driven by the growth of the Laurentide Ice Sheet) (see Yanase and Abe-Ouchi, 2007; 2010), combined with other factors, including an increase in extent and duration of sea ice, a reduction in global sea levels, a cooling of sea surface temperatures, and the localised growth of mountain glaciers.

**References**


Anders, A.M., Mitchell, S.G., Tomkin, J.H., 2010. Cirques, peaks, and precipitation patterns in the Swiss Alps: Connections among climate, glacial erosion, and topography. Geology 38(3), 239-242.

Aniya, M., Welch, R., 1981. Morphometric analyses of Antarctic cirques from photogrammetric measurements. Geografiska Annaler Series A 63 (1/2), 41-53.

ASTER GDEM Validation Team. 2011. ASTER Global Digital Elevation Model Version 2 – Summary of Validation Results. Available online at: http://www.ersdac.or.jp/GDEM/ver2Validation/Summary_GDEM2_validation_report_final.pdf.

Avdeiko, G.P., Savelyev, D.P., Palueva, A.A., Popruzhenko, S.V., 2007. Evolution of the Kurile-Kamchatkan volcanic arcs and dynamics of the Kamchatka-Aleutian junction. Geophysical Monograph Series – American Geophysical Union 172, 37-55.

Barr, I.D., Clark, C.D., 2011. Glaciers and climate in Pacific Far NE Russia during the Last Glacial Maximum. Journal of Quaternary Science 26 (2), 227-237.

Barr, I.D., Clark, C.D., 2012a. An updated moraine map of Far NE Russia. Journal of Maps, 8 (3), 1-6.

Barr, I.D., Clark, C.D., 2012b. Late Quaternary glaciations in Far NE Russia; combining moraines, topography and chronology to assess regional and global glaciation synchrony. Quaternary Science Reviews 53, 72-87.

Barr, I.D., Spagnolo, M., under review. Testing the efficacy of the glacial buzzsaw: insights from the Sredinny Mountains, Kamchatka.

Bigg, G. R., Clark, C.D., Hughes, A.L.C., 2008. A last glacial ice sheet on the Pacific Russian coast and catastrophic change arising from coupled ice–volcanic interaction. Earth and Planetary Science Letters 265 (3), 559-570.

Bindeman, I.N., Leonov, V.L., Izbekov, P.E., Ponomareva, V.V., Watts, K.E., Shipley, N., Perepelov, A.B., Bazanova, L.I., Jicha, B.R., Singer, B.S., Schmitt, A.K., Portnyagin, M.V., Chen, C.H., 2010. Large-volume silicic volcanism in Kamchatka: Ar–Ar and U–Pb ages, isotopic, and geochemical characteristics of major pre-Holocene caldera-forming eruptions. Journal of Volcanology and Geothermal Research 189 (1), 57-80.

Brook, M. S., Kirkbride, M. P., Brock, B. W., 2006. Cirque development in a steadily uplifting range: rates of erosion and long-term morphometric change in alpine cirques in the Ben Ohau Range, New Zealand. Earth Surface Processes and Landforms 31 (9), 1167-1175.

Cassie, B.E., Brigham-Grette, J., Lawrence, K.T., Herbert, T.D., Cook, M.S., 2010. Last Glacial Maximum to Holocene sea surface conditions at Umnak Plateau, Bering Sea, as inferred from diatom, alkenone, and stable isotope records. Paleoceanography 25, PA1206.

Chueca, J., Julián, A.,2004. Relationship between solar radiation and the development and morphology of small cirque glaciers (Maladeta Mountain massif, Central Pyrenees, Spain). Geografiska Annaler: Series A, Physical Geography 86(1), 81-89.

Davis, P.T., 1999. Cirques of the Presidential Range, New Hampshire, and surrounding alpine areas in the northeastern United States. Géographie physique et Quaternaire 53(1), 25-45.

Damiani, A.V., Pannuzi, L., 1987. La glaciazione pleistocenica nell'Appennino Laziale-Abruzzese. III nota: opportunità di precisazioni terminologiche, metodologiche ed introduzione di parametric morfometrici. Bollettino della Società Geologica Italiana 105 (1985–86), 75–96.

DeMets, C., Gordon, R.G., Argus, D.F., Stein, S., 1990. Current plate motions. Geophysical journal international 101 (2), 425-478.
Embleton, C., Hamann, C., 1988. A comparison of cirque forms between the Austrian Alps and the Highlands of Britain. Zeitschrift für Geomorphologie N.F. SupplementBand 70, 75-93.

Evans, I.S., 1977. World-Wide Variations in the Direction and Concentration of Cirque and Glacier Aspects. Geografiska Annaler Series A 59 (3/4), 151-175.

Evans, I.S., 1994. Lithological and structural effects on forms of glacial erosion: cirques and lake basins. In: Robinson, D.A., Williams, R.B.G. (eds.), Rock Weathering and Landform Evolution. John Wiley & Sons Ltd. Chichester. 455-472.

Evans, I.S., 1999. Was the cirque glaciation of Wales time-transgressive, or not?. Annals of Glaciology 28 (1), 33-39.

Evans, I.S., 2006a. Allometric development of glacial cirque form: geological, relief and regional effects on the cirques of Wales. Geomorphology 80 (3), 245-266.

Evans, I.S. 2006b. Local aspect asymmetry of mountain glaciation: a global survey of consistency of favoured directions for glacier numbers and altitudes. Geomorphology 73 (1), 166-184.

Evans, I.S., Cox, N.J., 1974. Geomorphometry and the operational definition of cirques. Area 6 (2), 150-153.

Evans, I.S., Cox, N.J., 1995. The form of glacial cirques in the English Lake District, Cumbria. Zeitschrift für Geomorphologie N.F. 39 (2), 175-202.

Evans, I.S., McClean, C.J., 1995. The land surface is not unifractal: variograms, cirque scale and allometry. Zeitschrift für Geomorphologie N.F. SupplementBand 101, 127–147.

Federici, P.R., Spagnolo, M., 2004. Morphometric Analysis on the Size, Shape and Areal Distribution of Glacial Cirques in the Maritime Alps (Western French-Italian Alps). Geografiska Annaler Series A *86* (3), 235-248.

Fedotov, S.A., Zolotarskaya, S.B., Maguskin, M.A., Nikitenko, Y.P., Sharoglazova, G.A., 1988. The study of deformations of the earth's surface on the Kamchatka Peninsula: repeated geodetic measurements. Journal of geodynamics 10 (2), 175-188.

Freitag, R., Gaedicke, C., Baranov, B., Tsukanov, N., 2001. Collisional processes at the junction of the Aleutian–Kamchatka arcs: new evidence from fission track analysis and field observations. Terra Nova 13 (6), 433-442.
Fu, P., Rich, P.M., 2002,. A geometric solar radiation model with applications in agriculture and forestry. Computers and Electronics in Agriculture 37 (1), 25-35.

García–Ruiz, J.M., Gómez–Villar, A., Ortigosa, L., Martí–Bono, C., 2000. Morphometry of glacial cirques in the Central Spanish Pyrenees. Geografiska Annaler Series A *82* (4), 433-442.

Gordon, J.E., 1977. Morphometry of cirques in the Kintail-Affric-Cannich area of northwest Scotland. . Geografiska Annaler Series A 59, 177-194.

Harker, A., 1901. Ice erosion in the Cuillin Hills, Skye. Transactions of the Royal Society of Edinburgh 40 (2), 221-252.

Hassinen, S., 1998. A morpho-statistical study of cirques and cirque glaciers in the Senja-Kilpisjärvi area, northern Scandinavia. Norsk geografisk Tidsskrift 52, 27-36.

Helland, A., 1877. On the Ice-Fjords of North Greenland, and on the Formation of Fjords, Lakes, and Cirques in Norway and Greenland. Quarterly Journal of the Geological Society 33 (1-4), 142-176.

Heyman, J., Stroeven, A., Caffee, M.W., Hättestrand, C., Harbor, J.M., Li, Y., Alexanderson, H., Zhou, L., Hubbard, A., 2011. Palaeoglaciology of Bayan Har Shan, NE Tibetan Plateau, exposure ages reveal a missing LGM expansion. Quaternary Science Reviews 30, 1988-2001.

Hijmans, R.J., Cameron, S.E., Parra, J.L., Jones, P.G., Jarvis, A., 2005. Very high resolution interpolated climate surfaces for global land areas. International journal of climatology *25* (15), 1965-1978.

Hourigan, J.K., Solov'ev, A.V., Ledneva, G.V., Garver, J.I., Brandon, M.T., Reiners, P.W., 2004. Timing of syenite intrusions on the eastern slope of the Sredinnyi Range, Kamchatka: Rate of accretionary structure exhumation. Geochemistry International 42 (2), 97-105.

Hughes, P.D., Gibbard, P.L., Woodward, J.C., 2007. Geological controls on Pleistocene glaciation and cirque form in Greece. Geomorphology 88 (3), 242-253.

Ivanov, A., 2002. The Far East. In: Shahgedanova, M. (Ed.), The Physical Geography of Northern Eurasia. Oxford University Press, Oxford pp. 422–447.

Kohfeld, K. E., Harrison, S. P., 2000. How well can we simulate past climates? Evaluating the models using global palaeoenvironmental datasets. Quaternary Science Reviews *19* (1), 321-346.

Křížek, M., Vočadlová, K., Engel, Z., 2012. Cirque overdeepening and their relationship to morphometry. Geomorphology 139-140, 495-505.

Krinner, G., Diekmann, B., Colleoni, F., Stauch, G., 2011. Global, regional and local scale factors determining glaciation extent in Eastern Siberia over the last 140,000 years. Quaternary Science Reviews 30 (7), 821-831.

Lehmkuhl, F., Owen, L.A., 2005. Late Quaternary glaciation of Tibet and the bordering mountains: a review. Boreas 34, 87-100.

Marinescu, E., 2007. The morphometry of the glacial cirques within the Gilort Basin. Analele Universității din Craiova. Seria Geografie 10, 5-12.

Matsumoto, T., Kodama, Y., Shiraiwa, T., Yamaguchi, S., Sone, T., Nishimura, K., Muravyev, Y. D., Khomentovsky, P. A., Yamagata, K., 1997. Meteorological observation by Automatic Weather Stations (AWS) in alpine regions of Kamchatka, Russia, 1996-1997. Low Temperature Science, Series A data report 56, 53-68.

McCall, J.G., 1960. The flow characteristics of a cirque glacier and their effect on glacial structure and cirque formation. In: Lewis, W.V. (Ed.), Norwegian Cirque Glaciers: Royal Geographic Society Research Series 4, pp. 39-62.

Mîndrescu, M., Evans, I.S., Cox, N.J., 2010. Climatic implications of cirque distribution in the Romanian Carpathians: palaeowind directions during glacial periods. Journal of Quaternary Science 25 (6), 875-888.

Nürnberg, D., Dethleff, D., Tiedemann, R., Kaiser, A., Gorbarenko, S.A., 2011. Okhotsk Sea ice coverage and Kamchatka glaciation over the last 350ka—Evidence from ice-rafted debris and planktonic $\delta^{18}O$. Palaeogeography, Palaeoclimatology, Palaeoecology 310 (3), 191-205.

Olyphant, G.A., 1981. Allometry and cirque evolution. Geological Society of America Bulletin 92 (9), 679-685.

Ono, Y., Aoki, T., Hasegawa, H., Dali, L., 2005. Mountain glaciation in Japan and Taiwan at the global Last Glacial Maximum. Quaternary International 138-139, 79-92

Otieno, F. O., Bromwich, D. H., Oglesby, R., 2012. Atmospheric circulation anomalies due to 115 kyr BP climate forcing dominated by changes in the North Pacific Ocean. Climate dynamics 38 (3), 815-835.

Persits, F.M., Ulmishek, G.F., Steinshouer, D.W., 1997. Maps showing geology, oil and gas fields and geologic provinces of the Former Soviet Union. USGS Open-File Report 97-470E.

Pinegina, T.K., Bourgeois, J., 2001. Historical and paleo-tsunami deposits on Kamchatka, Russia: long-term chronologies and long-distance correlations. Natural Hazards and Earth System Science 1 (4), 177-185.

Pedoja K, Bourgeois J, Pinegina T., 2004. Neotectonics near the NW corner of the Pacific Plate: terraces on Ozernoi and Kamchatskiy Peninsulas, Kamchatka, Russia (Abstract). In: IV International Biennial Workshop on Subduction Processes Emphasizing the Japan–Kurile Kamchatka–Aleutian Arcs. Petropavlovsk-Kamchatsky, 21-27 August 2004.

Pedoja, K., Bourgeois, J., Pinegina, T., Higman, B., 2006. Does Kamchatka belong to North America? An extruding Okhotsk block suggested by coastal neotectonics of the Ozernoi Peninsula, Kamchatka, Russia. Geology 34 (5), 353-356.

Péwé, T.L., Burbank, L., Mayo, L.R., 1967. Multiple glaciation of the Yukon-Tanana upland, Alaska. US Geological Survey. Misc. Geol. Invest. Map 1-105, scale 1/500,000.

Rudberg, S., 1994. Glacial cirques in Scandinavia, Norsk Geografisk Tidsskrift - Norwegian Journal of Geography 48 (4), 179-197.

Ruiz-Fernández, J., Poblete-Piedrabuena, M.A., Serrano-Muela, M.P., Martí-Bono, C., García-Ruiz, J.M., 2009. Morphometry of glacial cirques in the Cantabrian Range (Northwest Spain). Zeitschrift für Geomorphologie N.F. 53(1), 47-68.

Sawagaki, T., Aoki, T., 2011. Late Quaternary Glaciations in Japan. In: Ehlers, J., Gibbard, P.L., Hughes, P.D. (Eds.), Quaternary Glaciations - Extent and Chronology: A Closer Look. Developments in Quaternary Science 15. Elsevier, Amsterdam, pp. 1013-1022.

Sanders, J.W., Cuffey, K.M., Moore, J.R., MacGregor, K.R., Kavanaugh, J.L., 2012a. Periglacial weathering and headwall erosion in cirque glacier bergschrunds. Geology 40 (9), 779-782.

Sanders, J.W., Cuffey, K.M., MacGregor, K.R., Collins, B.D., 2012b. Sediment budget of an alpine cirque. Geological Society of America Bulletin 125 (1-2), 229-248.

Sauchyn, D.J., Cruden, D.M., Hu, X.Q., 1998. Structural control of the morphometry of open rock basins, Kananaskis region, Canadian Rocky Mountains. Geomorphology 22 (3), 313-324.

Savoskul, O. S., Zech, W., 1997. Holocene glacier advances in the Topolovaya Valley, Bystrinskiy Range, Kamchatka, Russia, dated by tephrochronology and lichenometry. Arctic and Alpine Research 29 (2), 143-155.

Shahgedanova, M., Perov, V., Mudrov, Y., 2002. The Mountains of Northern Russia. In: Shahgedanova, M. (Ed.), The Physical Geography of Northern Eurasia. Oxford University Press, Oxford, pp. 284-313.

Sharp, R.P., Allen, C.R., Meier, M.F., 1959. Pleistocene glaciers on southern California mountains. American Journal of Science 257(2), 81-94.

Stauch, G., Gualtieri, L., 2008. Late Quaternary glaciations in northeastern Russia. Journal of Quaternary Science *23* (6-7), 545-558.

Stauch, G., Lehmkuhl, F., 2010. Quaternary glaciations in the Verkhoyansk Mountains, Northeast Siberia. Quaternary Research 74 (1), 145-155.

Stauch, G., Lehmkuhl, F., Frechen, M., 2007. Luminescence chronology from the Verkhoyansk Mountains (North-Eastern Siberia). Quaternary Geochronology 2 (1), 255-259.

Steffanová, P., Mentlík, P., 2007. Comparison of morphometric characteristics of cirques in the Bohemian Forest. Silva Gabreta 13(3), 191-204.

Solomina, O., Wiles, G., Shiraiwa, T., D'Arrigo, R., 2007. Multiproxy records of climate variability for Kamchatka for the past 400 years. Climate of the Past 3 (1), 119-128.

Sone, T., Yamagata, K., Otsuki, Y., Sawada, Y., Vyatkina, M., 2006. Distribution of permafrost on the west slope of Mt. Ichinsky, Kamchatka, Russia. Bulletin of glaciological research 23, 6975.

Ureda, P., 2001. Glaciar relief and pleistocene glaciation in retezat mountains (Transylvanians Alps, Romania). Geographica Pannonica 5, 4-7.

Vilborg, L., 1984. The cirque forms of central Sweden. Geografiska Annaler. Series A. Physical Geography 66(1-2), 41-77.

Yanase, W., Abe-Ouchi, A., 2007. The gLGM surface climate and atmospheric circulation over East Asia and the North Pacific in the PMIP2 coupled model simulations. Climate of the Past 3 (3), 439-451.

Yanase, W., Abe-Ouchi, A., 2010. A numerical study on the atmospheric circulation over the midlatitude North Pacific during the last glacial maximum. Journal of Climate, 23(1), 135-151.